Proceedings of the 2005 IEEE
International Conference on Robotics and Automation
Barcelona, Spain, April 2005

Haptic Interface using Delayed Reflection Wave: Application to a Passive Haptic Device

Jae-Hyeong Lee, Chang-Hyun Cho and Jae-Bok Song
Dept. of Mechanical Engineering
Korea University
Anam-dong, Seongbuk-gu, Seoul, 136-701, Korea
quarky@korea.ac.kr

Chang-Soon Hwang and Munsang Kim
Intelligent Robotics Research Center
Korea Institute of Science and Technology
Hawolgok-dong, Seongbuk-gu, Seoul, 136-791, Korea
cshwang@kist.re.kr

Abstract **- It is well known that the wave variables are robust to time delay of a system from the viewpoint of passivity. During implementation of the wave transformation on the sampled-data system, a unit time delay arises due to causality of the reflection wave. The unit time delay on the reflection wave occasionally becomes a passive element. From the passivity condition of the sampled-data system, the wave impedance can be designed such that the wave transformation using delayed reflection provides the effect of positive damping and thus the stable haptic interface is achieved on the sampled-data system. Various experiments for a 2-linked passive haptic device show that stable haptic interface can be accomplished for the wall-following task by use of the wave transformation using delayed reflection.**

Index Terms – Delayed reflection wave, Haptic interface, Sampled-data system, Wave variables.

I. INTRODUCTION

The wave transformation or wave variables have been widely used to deal with time delay in bilateral teleoperation [1][2][3]. The wave impedance that determines the behavior of a transmission line is an essential parameter in the wave transformation. However, much attention has not been paid to the design issue of the wave impedance. It is generally known that a haptic interface on the sampled-data system sometimes exhibits unstable behavior especially when a large amount of power is involved (e.g., the high stiffness wall). The wave transformation for the sampled-data system has a unit time delay for the causality due to the reflection wave. The unit time delayed reflection wave can be a passive or an active element depending on the choice of the wave impedance. Therefore, the wave impedance can be designed such that the unit time delayed reflection wave represents a positive damping element.

Anderson and Spong suggested a delayed transmission line that was designed for bilateral teleoperation based on the passivity and scattering theory. In the transmission line, the norm of the scattering matrix was one, and there was no loss [4]. Niemeyer and Slotine showed that the time delay was not an active element in the wave space that consisted of wave variables [1]. The wave variables stemmed from the scattering parameter which was the ratio of the reflected power wave to the incident power wave [5]. Wave variables were mainly used to deal with time delay for bilateral teleoperation [2][3].

Colgate and Schenkel found the passivity condition for haptic interface in the sampled-data system that made the virtual wall active [6][7]. Hannaford and Ryu suggested the passivity controller based on the passivity observer in the time domain [8]. Most researches on haptic interfaces have focused on designing the fixed or varying virtual coupling [9][10][11].

Some researchers have applied the concept of wave variables to the haptic interface. In the haptic interface, there are several active elements such as time delay due to numerical integration and sampling and quantization related to the discrete-time system. The unit time delayed reflection wave in the wave space is occasionally a passive element depending on the choice of the wave impedance with the other parameters fixed. This paper aims at designing the wave impedance that make the haptic interface stable through the wave transformation using delayed reflection. Using the passivity condition for the conventional haptic interface, one can find the condition of the wave impedance that makes the unit time delay a passive element or a positive damping element. The experiments using a 2-linked passive haptic device showed that the haptic interface through the wave transformation using delayed reflection could produce satisfactory performance for the wall-following task on the virtual environment.

Section 2 introduces the wave variables, and Section 3 deals with the basic haptic interface, the fundamental limits of conventional haptic interface and the condition for the passive interface. The wave transformation and the passivity condition for the sampled-data system are discussed in Section 4. In section 5, the stable haptic interface is extended to a passive haptic system and experimental results are presented. Finally, the conclusions are drawn in Section 6.

II. WAVE TRANSFORMATION

A. Definition

Wave variables are designed on the basis of the passivity and scattering parameters in the network theory [2]. From the viewpoint of passivity, the wave variables are robust to arbitrary time delays. Figure 1 illustrates time delayed transmission of wave variables. The wave variables are defined as

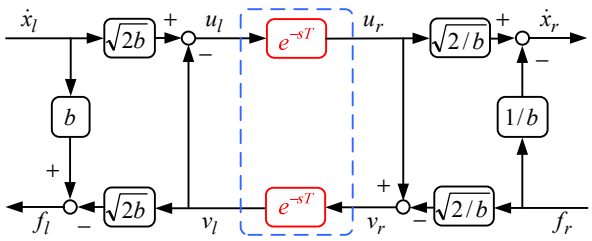

Fig. 1 Time-delayed transmission through the wave transformation.

$$\begin{bmatrix} u \\ v \end{bmatrix} = \begin{bmatrix} 1/\sqrt{2b} & \sqrt{b/2} \\ -1/\sqrt{2b} & \sqrt{b/2} \end{bmatrix} \begin{bmatrix} f \\ \dot{x} \end{bmatrix} \tag{1}$$

where the wave impedance b is an arbitrary constant which determines the behavior of the transmission line, $\dot{x}$ and f are the velocity and force, u and v are the forward and backward waves, respectively. The subscripts l and r denote the left and right ports. Since the transformation is one-to-one, the inverse of (1) is uniquely determined as

$$\begin{bmatrix} f \\ \dot{x} \end{bmatrix} = \begin{bmatrix} \sqrt{b/2} & -\sqrt{b/2} \\ 1/\sqrt{2b} & 1/\sqrt{2b} \end{bmatrix} \begin{bmatrix} u \\ v \end{bmatrix} \tag{2}$$

B. Property of time-delayed transmission through wave transformation

From Fig.1, the time-delayed transmission can be represented in the input-output vector form as

$$\begin{bmatrix} f_l \\ -\dot{x}_r \end{bmatrix} = O(s) := H(s)I(s) = \begin{bmatrix} \frac{b(1-e^{-2sT})}{1+e^{-2sT}} & \frac{2e^{-sT}}{1+e^{-2sT}} \\ -\frac{2e^{-sT}}{1+e^{-2sT}} & \frac{1-e^{-2sT}}{b(1+e^{-2sT})} \end{bmatrix} \begin{bmatrix} \dot{x}_l \\ f_r \end{bmatrix} \tag{3}$$

where $I(s)$, $O(s)$, and $H(s)$ are the input vector, output vector and hybrid transformation matrix, respectively. From linear system theory and network theory, the passivity condition of a system can be written as

$$H(s) + H^*(s) \geq 0, \quad \forall \omega \geq 0, \tag{4}$$

$$\left\| (H(s) - I)(H(s) + I)^{-1} \right\| \leq 1 \quad \forall \omega. \tag{5}$$

That is, a hermitian matrix needs to be positive semi-definite in the right half of the s-plane and the norm of the scattering matrix is less than or equal to 1. From (3), the hermitian matrix of $H(s)$ is positive semi-definite and the norm of the scattering matrix of $H(s)$ is equal to 1, so the time-delayed transmission satisfies the passivity condition. Therefore the time-delayed transmission is not only passive but also lossless.

III. Basic Haptic Interface

A. Definition

Figure 2 illustrates a simple haptic interface in which the haptic device and virtual environment are modeled by the mass m_d and the spring K_{ve}, respectively. The haptic device is moved by the human force f_h. When the device is in contact with the virtual environment, the reaction force f_{ve} can be computed as the product of the spring stiffness, K_{ve}, and the displacement of the virtual spring, x_{ve}. This reaction force is transmitted to the operator through the haptic device. In the figure, the superscript * denotes the discrete-time signal.

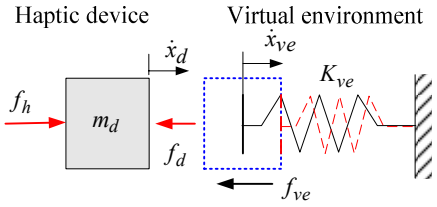

Fig. 2 Schematic of a basic haptic interface.

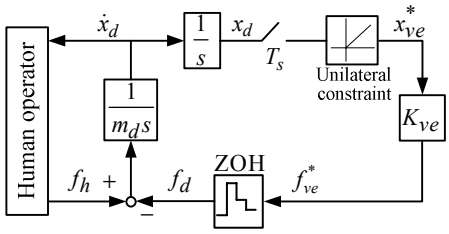

Fig. 3 Basic haptic interface on sampled-data system.

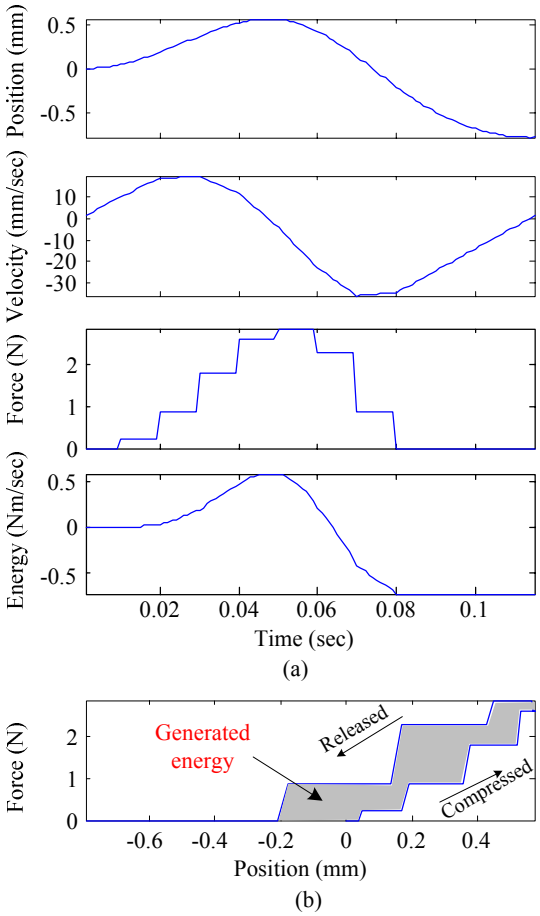

Fig. 4 Example of basic haptic interface (K_{ve}=5kN/m, T=10^{-2}sec, m_d=1kg and f_h=1N).

The dynamics of the haptic device and virtual environment can be written as

$$m_d \frac{d}{dt}\dot{x}_d(t) = f_h(t) - f_d(t) \tag{6}$$

$$K_{ve}\int_0^t \dot{x}_{ve}(\tau)d\tau = f_{ve}(t) \tag{7}$$

where f_d is the transmitted force from the virtual environment to the haptic device, and $\dot{x}_d$ and $\dot{x}_{ve}$ are the

velocities of the haptic device and virtual environment, respectively. In the case of the haptic device in contact with the virtual environment, $\dot{x}_d = \dot{x}_{ve}$ and $f_d = f_{ve}$. Therefore, the dynamics of the haptic interface can be represented as

$$m_d \frac{d}{dt}\dot{x}_{ve}(t) + K_{ve}\int_0^t \dot{x}_{ve}(\tau)d\tau = f_h(t) \tag{8}$$

Equation (8) is a simple mass-spring system. It is generally known that the ideal haptic interface based on (8) is passive and lossless.

B. Active wall

In practice, the virtual environment cannot be composed of only linear components. The basic haptic interface of Fig. 2 can be implemented in Fig. 3 using nonlinear elements such as a sampler, ZOH and unilateral constraint. Figure 4 depicts a simple numerical computation for the system of Fig. 3. Assume that the initial position of the haptic device is placed zero in front of the virtual wall. The stored energy becomes negative when the virtual spring is released and this negative energy causes the displacement to increase and the force to change more rapidly than that during compression.

The source of negative energy can be found from force-displacement curves as shown in Fig. 4(b). In the ideal spring, the amount of energy stored in the spring by compression is removed by the same amount during release. The virtual spring implemented in discrete-time, the curve has a kind of hysteresis. Since the force during release becomes greater than that during compression, the spring generates more energy during release than it receives during compression. In this case, the spring acts as an active wall [7]. The passivity of the sampled-data system can be verified by

$$b_d > \frac{T}{2}(1-\cos\omega T)^{-1}\,\mathrm{Re}\{(1-e^{-j\omega T})H_{ve}(e^{j\omega T})\} \tag{9}$$

where b_d is the viscous friction of the haptic device, and $H_{ve}(e^{j\omega T})$ is the transfer function of the virtual environment [6]. As an example, when (9) is applied to the system of Fig. 3, the system is passive if and only if $K_{ve}T < 0$, but it is impossible to satisfy this condition, since $K_{ve}>0$ and $T>0$. Hence, the system is intrinsically active.

IV. Wave Transformation using Delayed Reflection

A. Wave transformation on sampled-data system

The concept of wave variables can be used in bilateral teleoperation with time delay. However, little research has been done on the application of wave transformation to haptic interfaces to overcome the problems associated with the active wall. Since the wave transform is intrinsically passive, it is desirable to design a haptic interface in wave space when time delay exists. For the practical implementation of the wave transformation for the sampled-data system shown in Fig. 5, the term of reflection wave should include the unit delayed wave variables. This is called wave transformation using the unit time delayed wave reflection or simply the wave transformation using delayed reflection.

The wave variables in Fig. 5 can be written as

$$\begin{bmatrix} u \\ v \end{bmatrix} = \begin{bmatrix} e^{-sT}/\sqrt{2b} & (2-e^{-sT})\sqrt{b/2} \\ -1/\sqrt{2b} & \sqrt{b/2} \end{bmatrix} \begin{bmatrix} f_d \\ \dot{x}_d \end{bmatrix} \tag{10}$$

$$\begin{bmatrix} u \\ v \end{bmatrix} = \begin{bmatrix} 1/\sqrt{2b} & \sqrt{b/2} \\ -(2-e^{-sT})/\sqrt{2b} & e^{-sT}\sqrt{b/2} \end{bmatrix} \begin{bmatrix} f_{ve} \\ \dot{x}_{ve} \end{bmatrix} \tag{11}$$

where $\dot{x}$ and f are the velocity and force, respectively. The subscripts d and ve denote the haptic device and virtual environment, respectively, and T is the sampling period of the system. The inverses of (10) and (11) are given uniquely by

$$\begin{bmatrix} f_d \\ \dot{x}_d \end{bmatrix} = \begin{bmatrix} e^{-sT}/\sqrt{2b} & (2-e^{-sT})\sqrt{b/2} \\ -1/\sqrt{2b} & \sqrt{b/2} \end{bmatrix} \begin{bmatrix} u \\ v \end{bmatrix} \tag{12}$$

$$\begin{bmatrix} f_{ve} \\ \dot{x}_{ve} \end{bmatrix} = \begin{bmatrix} 1/\sqrt{2b} & \sqrt{b/2} \\ -(2-e^{-sT})/\sqrt{2b} & e^{-sT}\sqrt{b/2} \end{bmatrix} \begin{bmatrix} u \\ v \end{bmatrix} \tag{13}$$

From (10) and (11), or (12) and (13), the transfer matrix of the wave transformation using delayed reflection can be written as

$$\begin{bmatrix} f_d \\ -\dot{x}_{ve} \end{bmatrix} = O(s) := H(s)I(s) = \begin{bmatrix} \dfrac{b(1-e^{-sT})^2}{1+e^{-2sT}} & \dfrac{2}{1+e^{-2sT}} \\ -\dfrac{2}{1+e^{-2sT}} & \dfrac{(1-e^{-sT})^2}{b(1+e^{-2sT})} \end{bmatrix} \begin{bmatrix} \dot{x}_d \\ f_{ve} \end{bmatrix} \tag{14}$$

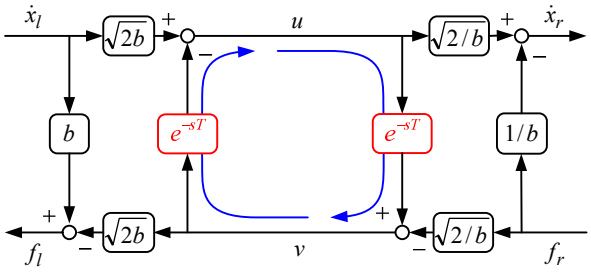

Fig. 5 Wave transformation using delayed reflection.

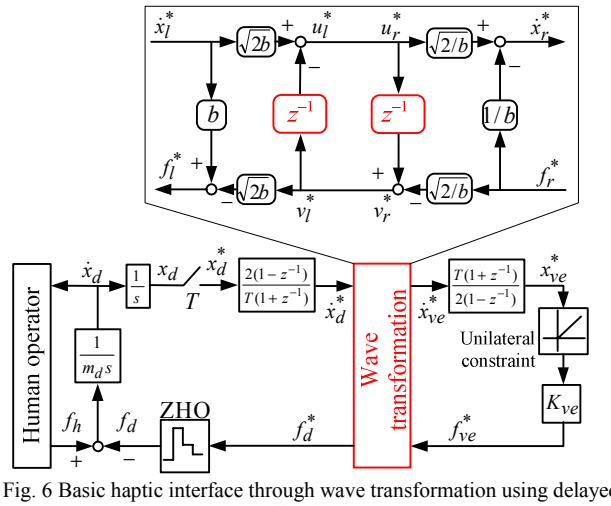

Fig. 6 Basic haptic interface through wave transformation using delayed reflection.

B. Passivity condition for haptic interface

When the wave transformation using delayed reflection is applied to the basic haptic interface, the whole system can be represented in Fig. 6. From Fig. 6, the velocity and force of the virtual environment have relation as following

$$f_{ve}^{*} = K_{ve}\frac{T(1+e^{-sT})}{2(1-e^{-sT})}\dot{x}_{ve}^{*} \tag{15}$$

where $z = e^{sT}$. From (14), the relation of the power variables between the haptic device and the virtual environment can be written as following

$$\begin{bmatrix} f_d^* \\ \dot{x}_d^* \end{bmatrix} = \frac{1}{2}\begin{bmatrix} 1+(2-e^{-sT})^2 & b(1-e^{-sT})^2 \\ (1-e^{-sT})^2/b & 1+e^{-2sT} \end{bmatrix}\begin{bmatrix} f_{ve}^* \\ \dot{x}_{ve}^* \end{bmatrix} \tag{16}$$

Combining (15) and (16), the transfer function of the virtual environment which includes the wave transformation can be obtained as following (without the unilateral constraint)

$$H_{ve}(e^{sT}) = \frac{4b^2(1-e^{-sT})^4 + 4bK_{ve}T(1-e^{-2sT})(1+(2-e^{-sT})^2)}{2bT(1-e^{-4sT}) + K_{ve}T^2(1-e^{-2sT})^2} \tag{17}$$

where, $H_{ve} = f_d^*/\dot{x}_d^*$. To verify the passivity of the system, applying the transfer function (16) to the passivity condition of (9) gives

$$Q(b,\omega) = \frac{2(K_{ve}T-2b)(K_{ve}T+(K_{ve}T-2b)\cos(\omega T))}{4b^2+K_{ve}{}^2T^2+(4b^2-K_{ve}{}^2T^2)\cos(2\omega T)} - 1 < 0 \tag{18}$$

where, $0 \le \omega \le \pi/T$. The critical points of the function $Q(b,\omega)$ can be found for the boundary values and the values satisfying $\partial Q/\partial\omega = 0$ as follow:

$$\frac{K_{ve}T(K_{ve}T-3b)}{2b^2} \tag{19}$$

$$\frac{4b^2-8bK_{ve}T-K_{ve}^2T^2-4K_{ve}T\sqrt{b(2b+K_{ve}T)}}{2K_{ve}T(2b+K_{ve}T)+4K_{ve}T\sqrt{b(2b+K_{ve}T)}} \tag{20}$$

$$\frac{4b^2-8bK_{ve}T-K_{ve}^2T^2+4K_{ve}T\sqrt{b(2b+K_{ve}T)}}{2K_{ve}T(2b+K_{ve}T)-4K_{ve}T\sqrt{b(2b+K_{ve}T)}} \tag{21}$$

$$\frac{K_{ve}T-4b}{2b} \tag{22}$$

From the critical points, the maximum values of the function $Q(b,\omega)$ are

$$\frac{K_{ve}T(K_{ve}T-3b)}{2b^2}, \quad \text{where } 2b < K_{ve}T \tag{23}$$

$$\frac{4b^2-8bK_{ve}T-K_{ve}^2T^2-4K_{ve}T\sqrt{b(2b+K_{ve}T)}}{2K_{ve}T(2b+K_{ve}T)+4K_{ve}T\sqrt{b(2b+K_{ve}T)}}, \quad \text{where } 2b > K_{ve}T \tag{24}$$

If the maximum value of $Q(b,\omega)$ is less than zero, the haptic interface through the wave transformation using delayed reflection is passive. From (23) and (24), the maximum value of $Q(b,\omega)$ is less than zero over the entire frequency range where

$$0.333 < b/(K_{ve}T) < 3.579 \tag{25}$$

Figure 7 shows the graph for $Q(b,\omega)$) over frequency with K_{ve} = 1kN/m and T =1msec. If the passivity condition is applied to the system of Fig. 6, the haptic interface becomes passive as shown in Fig. 8. The parameters used in this simulation are the same as those of Fig. 4 except for K_{ev} and T. The initial position of the haptic device is placed at zero and the virtual wall is placed at −0.1 m. From (25) and the value of $K_{ve}T$, the wave impedance used in the simulation was set to 35 Nsec/m.

It follows from the simulation results that the wave transformation using delayed reflection with the appropriate wave impedance can make the haptic interface stable. The position, velocity, and force responses in Fig. 8 indicate the stable behavior of the haptic interface. Note that the stored energy is kept positive at all times. In the steady state, the wave variables had the same magnitude but the opposite sign. Their magnitude is $0.118\sqrt{\text{Nm/sec}}$.

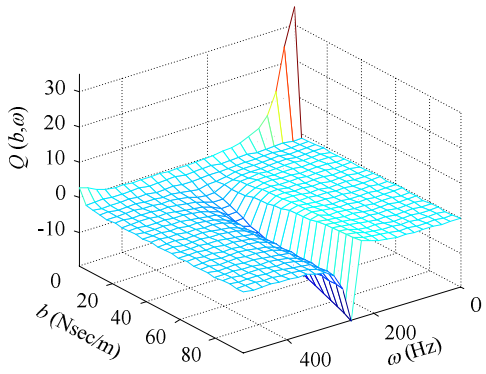

Fig. 7 $Q(b, \omega)$ as a function of frequency and wave impedance.

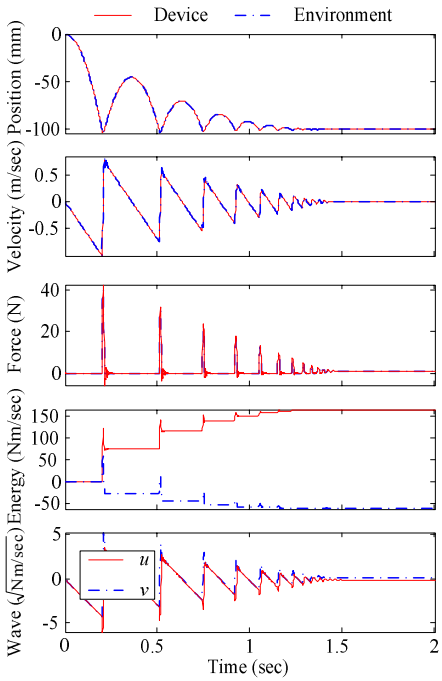

Fig. 8 Simulation results
(K_{ve}=10^{4}N/m, T=10^{-3}sec, m_d=1kg and f_h=1N, b=35Nsec/m).

V. EXPERIMENTS FOR PASSIVE HAPTIC DEVICE

In the previous section, it was shown that the haptic interface using wave variables can be intrinsically passive depending on the choice of the wave impedance. In the haptic interface, the only difference between the passive and the active haptic device is where to employ is the force approximation in the haptic controller for passive haptic device. Through the passive FME (Force Manipulability Ellipsoid) analysis [12], pullback motion can be analyzed, in which the end-effector can be brought back to the wall surface once it penetrates into the wall. However, the force approximation makes the pullback motion partially available for a passive haptic device. A haptic system using the passive haptic device exhibits unstable behavior such as unsmooth motion, when it has the pullback capability due to force approximation [12]. To obtain a stable haptic interface, the proposed haptic interface in Fig. 6 is applied to the haptic system using the passive haptic device.

The 2-link passive haptic device equipped with 2 electric brakes shown in Fig. 9 was constructed for experiments. The angles θ_i and θ_{Bi} represent the joint angle and the rotating angle of the brake, respectively, and k_i is the reduction ratio of the tendon-drive system. The design parameters are $k_2 = 0.4$ and $l_1 = l_2 = 0.15$m. Brake 1 (or 2) which provides a braking torque to link 1 (or 2) is mounted at the base and conveys the torque through pulleys P_{1a}-P_{1b} (or P_{2a}-P_{2b}). In this situation, θ_2 is computed by

$$\theta_2 = k_2\theta_{B2} - k_2\theta_1 \tag{26}$$

Note that θ_2 is a function of θ_1 as well as θ_{B2}. That is, the coupled motion [13] in the wire transmission is observed in θ_2. Placing both brakes at the base has an advantage of reducing the mass of the moving part. Rotational motion of each brake is sensed by the optical encoder mounted on the brake axis.

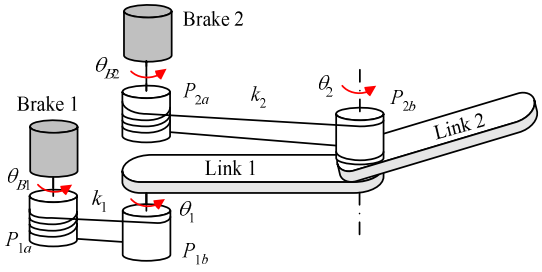

Fig. 9 Coupled tendon-drive mechanism.

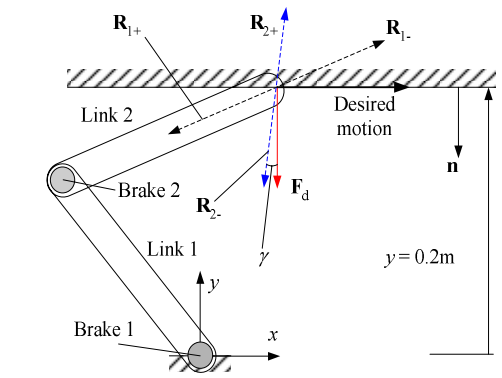

Fig. 10 Location of virtual wall and experimental conditions.

A brake can generate its braking torque only in the passive region in which $\tau \cdot \dot{q} \le 0$ is satisfied, where $\dot{q}$ and τ are the joint velocity and joint torque, respectively. Let $\mathbf{J}$ be the Jacobian matrix and $\mathbf{J}_i$ be the ith column vector of $\mathbf{J}^{-T}$ = $[\mathbf{J}_1 \cdots \mathbf{J}_n]$. From $\mathbf{F}=\mathbf{J}(\mathbf{q})^{-T}\boldsymbol{\tau}$, we can obtain available forces corresponding to joint conditions (e.g., $\dot{q}_i$) by adopting the Karnopp's stick-slip model [14] as follows:

$$\mathbf{R}_i = -\mathrm{sgn}(\dot{\theta}_i)\mathbf{J}_i, \quad \dot{\theta}_i \neq 0 \qquad \text{(Slip mode)} \tag{27}$$

$$\mathbf{R}_i = -\mathrm{sgn}(\tau_{hi})\mathbf{J}_i, \quad \dot{\theta}_i = 0 \qquad \text{(Stick mode)} \tag{28}$$

where the subscript i denotes the joint number and τ_{hi} represents the hand torque input. In this paper $\mathbf{R}_i$ is termed as the reference force.

Figure 10 shows experimental conditions. Two brakes generated a braking torque in proportion to the input current at a rate of 1kHz. The plane virtual wall located at y = 0.2m was modeled as a spring whose spring constant was 10^4N/m, but it was assumed to possess neither damping nor friction on the surface. The wave impedance was set to 36Nm/sec. The experimental conditions were the same as in numerical simulations except for use of the passive haptic device. A hand force input was provided to move the handle mounted at the end-effector in the $+x$ direction while it maintained contact with the virtual wall. In order to accomplish this wall-following task, the haptic device is required to display the desired force $\mathbf{F}_d$ normal to the virtual surface. Since the brake can generate a torque only against its rotation or against the externally applied torque, however, even a combination of two brake torques cannot accurately display this force in this case, which can be easily detected from FME analysis. Hence, the reaction force $\mathbf{F}_d$ can be displayed approximately at most by $\mathbf{R}_{2-}$ which was obtained with brake 2 activated and brake 1 fully released.

Various experiments based on the wave transformation have been carried out. Figure 11 shows the schematic of the signal flows of the passive haptic interface through wave transformation. The approximate force from the passive FME and the haptic device velocity were transmitted through wave transformation, which is only different from the conventional interface based on a passive haptic device. In the experiment results shown in Fig. 11, smooth paths of the end-effecter were observed after the first contact with the virtual wall for the proposed haptic interface. The penetration depth also remained at a relatively constant value, whereas unsmooth motion (i.e., contact and non-contact) was repeated with the conventional interface. It was shown that the y velocity stayed around zero after contacting the wall. Some oscillation was observed because the wave transformation was sensitive to the velocity noise, but the magnitude rapidly decreased. Furthermore, no sudden change that frequently occurred at the conventional interface was observed on the curve of the desired force.

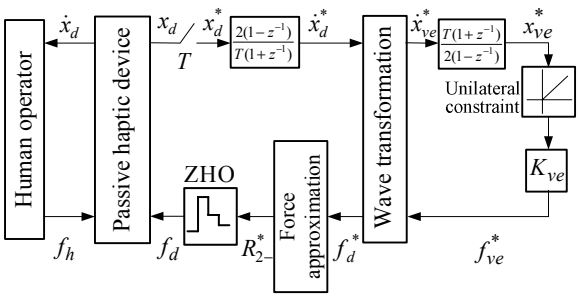

Fig. 11 Haptic interface based on a passive haptic device through wave transformation.

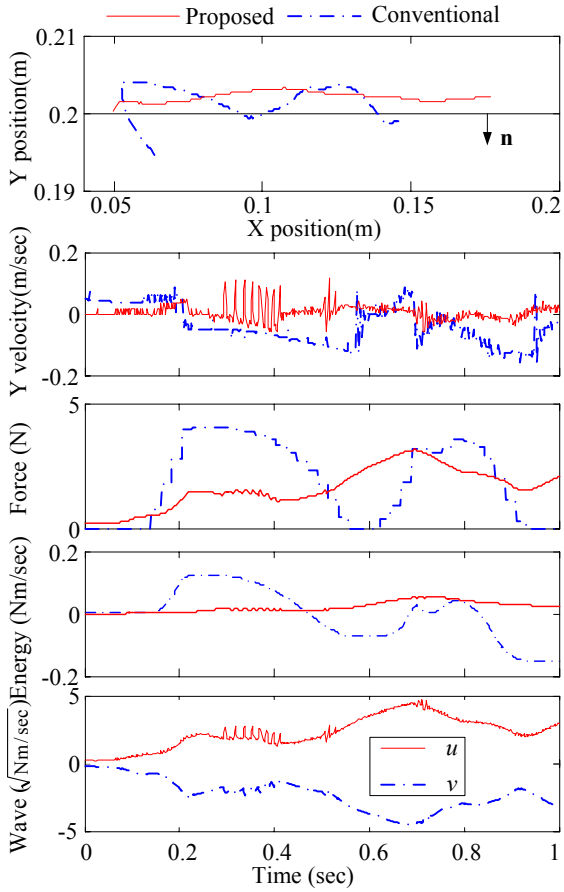

Fig. 12 Experimental results using wave transformation ($T = 10^{-3}$sec, $K = 10^{4}$N/m, and $b = 35$Nsec/m).

The energy of the system is worth discussion. The stored energy became negative from time to time for the conventional haptic interface, whereas it remains positive for the proposed haptic interface, thus meaning that the system is passive all the time. It is noted that the wave variables of the ideal display will remain at a constant value after the initial contact, since there is no change of the device velocity and the environment force. It is also observed in Fig. 12 that the wave variables had the same magnitudes but the opposite sign at the steady state, which indicated that the haptic interface was stable.

VI. Conclusions

In this paper, the wave transformation was implemented on the sampled-data system. For this implementation, the unit time delayed reflection wave is a necessary component. The wave transformation using delayed reflection could be either an active or a passive element according to the wave impedance. From the passivity condition of the sampled-data system, the wave impedance can be found which makes the wave transformation using delayed reflection a positive damping. As an example, the wave transformation using delayed reflection can make the haptic interface stable on the sampled-data system without additional damping.

The experiments for the passive haptic device also show that the stable haptic interface can be accomplished using the wave transformation. As a result, it is shown that the wave transformation using delayed reflection is intrinsically a control law. Therefore the wave transformation is beneficial not only to the bilateral teleoperation with time delay, but also to the haptic interface implemented in the sampled-data form.

References

[1] G. Niemeyer and J. J. Slotine, "Stable Adaptive Teleoperation," *IEEE Journal of Oceanographic Engineering*, vol. 16, no. 1, 1991, pp.152-162.

[2] S. Munir and W. J. Book, "Internet-Based Teleoperation Using Wave Variables with Prediction," *IEEE/ASME Trans. on Mechatronics*, vol. 7, no. 2, pp.124-133, June 2002.

[3] Y. Yokokohji, T. Imaida and T. Yoshikawa, "Bilateral Teleoperation under Time-Varying Communication Delay," in *Proc. The IEEE/RSJ Int. Conf. on Intelligent Robots and Systems*, Kyongju, Korea, 1999, pp.1854-1859.

[4] R.J. Anderson and M.W. Spong, "Bilateral Control of Teleoperators with Time Delay," *IEEE Trans. on Automatic Control*, vol. 34, no. 5, 1989, pp.494-501.

[5] S. S. Haykin, *Active Netwok Theory*, Addison-Wesley, 1970.

[6] J. E. Colgate, P. E. Grafing, M.C. Stanley and G. Schenkel, "Implementation of stiff virtual walls in force-reflecting interfaces," in *Proc. The IEEE Virtual Reality Annual International Symposium*, 1993, pp.202-208.

[7] J. E. Colgate and G. G. Schenkel, "Passivity of a Class of Sampled-Data Systems: Application to Haptic Interface," *Journal of Robotic System,* vol. 14, no. 1, 1997, pp.37-47.

[8] B. Hannaford and J-H. Ryu, "Time-Domain Passivity Control of Haptic Interface," *IEEE Trans. on Robotics and Automation*, vol. 18, no. 1, 1999, pp.1-10.

[9] R. Daniel and P. McAree, "Fundamental limits of performance for force reflecting teleoperation," *International Journal of Robotics Research,* vol. 7, no. 8, 1998, pp.811-830.

[10] R. J. Adams, and B. Hannaford, "Stable Haptic Interface with Virtual environment," *The International Journal of Robotics Research,* vol. 17, no. 8, 1999, pp.811-830.

[11] S. E. Salcudean, M. Zhu, W-H. Zhu and K. Hashtrudi-Zaad, "Transparent Bilateral Teleoperation under Position and Rate Control," *IEEE Trans. on Robotics and Automation*, vol. 15, no. 3, 2000, pp.465-474.

[12] C. H. Cho, J. B. Song, M. S. Kim and C.S. Hwang, "Energy-Based Control of a Passive Haptic Device," in *Proc. The IEEE Int. Conf. on Robotics and Automation*, New Orleans, LA, 2004, pp. 292-297.

[13] S. Ma, H. Yoshinada and S. Hirose, "CT ARM-I: coupled tendon-driven manipulator model I-design and basic experiments," in *Proc. The IEEE Robotics and Automation*, Nice, France, vol. 3, 1992, pp.2094-2100.

[14] D. Karnopp, "Computer simulation of stick-slip friction in mechanical dynamic system," *ASME Journal of Dynamic Systems, Measurement, and Control*, vol. 107, 1985, pp.100-103.